JOURNAL OF GEOPHYSICAL RESEARCH, VOL. 112, D22204, doi:10.1029/2007JD008974, 2007

MODIS derived fine mode fraction characteristics of marine, dust, and anthropogenic aerosols over the ocean, constrained by GOCART, MOPITT, and TOMS

Thomas A. Jones[1] and Sundar A. Christopher[1]

Received 15 May 2007; revised 26 July 2007; accepted 22 August 2007; published 29 November 2007.

[1] One year (December 2003 to November 2004) of Terra Moderate Resolution Imaging Spectroradiometer (MODIS), Total Ozone Mapping Spectrometer (TOMS), and Measurement of Pollution in the Troposphere (MOPITT) data over the open ocean are used in conjunction with the Goddard Chemistry Transport Model (GOCART) to characterize differing aerosol types as a function of satellite observable parameters. GOCART model output is used to select regions that are dominated (at least 80% of the total aerosol optical thickness from a single aerosol species) by anthropogenic (black carbon + organic carbon + sulfate), dust (DU) and sea salt regions (SS). Aerosol optical thickness (AOT) and fine mode fraction (FMF) retrieved from MODIS are averaged for each aerosol species region at 1 month intervals to examine the observational differences among each aerosol species. Anthropogenic (AN) aerosols are further separated into those produced primarily from biomass burning (BB) versus those from combustion and industrial pollution (PO). TOMS ultraviolet absorbing aerosol index (AI) in conjunction with MOPITT carbon monoxide (CO) data sets on Terra are used to contrast the differences between BB and PO aerosol properties. Annually averaged estimates for SS, DU, and AN MODIS FMF are 0.25 ± 0.07, 0.45 ± 0.05, and 0.84 ± 0.04, respectively, in agreement with or slightly lower than previous estimates. However, FMF values were observed to change substantially as a function of space and time as regions dominated by single aerosol types shrink, expand, and move around from month to month. The greatest variability in FMF was observed for SS and DU aerosols. SS are associated with regions of high near-surface wind speeds in the Southern Hemisphere, which have large temporal and spatial variations. Dust transport off of the Saharan Desert is maximized in the Northern Hemisphere summer, increasing the area of predominately dust aerosols. MODIS aerosol effective radius for each aerosol type also showed a similar trend with SS, DU, and AN values of 1.03, 0.68, and 0.32 μm. TOMS-AI values for DU exceeded SS and AN values up to 100% between April and October 2004 in association with the greatest dust concentrations in the North Atlantic. For BB and PO components of AN aerosols, no significant difference in MODIS FMF were observed; however, substantial differences in TOMS-AI and MOPITT values were observed between BB and PO aerosols, especially between June and November. For both TOMS-AI and MOPITT CO, BB aerosols are generally associated with higher values than are PO aerosols. The use of GOCART to constrain regions where a dominant aerosol species exists has allowed a comprehensive analysis of the satellite observed properties of various aerosol species.

Citation: Jones, T. A., and S. A. Christopher (2007), MODIS derived fine mode fraction characteristics of marine, dust, and anthropogenic aerosols over the ocean, constrained by GOCART, MOPITT, and TOMS, *J. Geophys. Res.*, *112*, D22204, doi:10.1029/2007JD008974.

1. Introduction

[2] The importance of tropospheric aerosols on the radiative balance of the Earth-atmosphere system has been examined by numerous studies (see *Yu et al.* [2006] for a comprehensive review). Using satellite data, recent research has attempted to quantify the relationship between anthropogenic [*Bellouin et al.*, 2005; *Christopher et al.*, 2006] and

[1]Department of Atmospheric Sciences, University of Alabama in Huntsville, Huntsville, Alabama, USA.

0148-0227/07/2007JD008974$09.00

Table 1. Fine Mode Fraction Values for Sea Salt (F_{ma}), Dust (F_{du}), and Anthropogenic (F_{an}) Aerosols Derived From *Kaufman et al.* [2005a, 2005b], *Bellouin et al.* [2005], and This Research[a]

F_{ma}	F_{du}	F_{an}	Research
0.30 ± 0.10	0.50 ± 0.05	0.90 ± 0.05	*Kaufman et al.* [2005a]
0.32 ± 0.07	0.51 ± 0.03	0.92 ± 0.03	*Kaufman et al.* [2005b]
0.35 ± 0.05	NA	0.83 ± 0.05	*Bellouin et al.* [2005]
0.25 ± 0.09	0.44 ± 0.06	0.83 ± 0.04	this research

[a]Note that *Bellouin et al.* [2005] combines sea salt and dust aerosols into "naturally occurring" aerosols.

dust aerosols [e.g., *Christopher and Jones*, 2007] on top of atmosphere (TOA) shortwave radiative effects. Anthropogenic (AN) aerosols are primarily from (1) biomass burning (BB) and (2) fossil fuel combustion in power generation/vehicles [*Chin et al.*, 2004] that we collectively call pollution aerosols (PO). Aerosols with anthropogenic characteristics can also result from natural sources such as naturally occurring forest fires and emission of dimethyl sulfide (DMS) from biological sources. However, their contribution to the total AOT in heavily polluted regions is small.

[3] Various methods have been used to separate total column aerosol optical thickness at 0.55 μm (AOT) by aerosol type. Using the Moderate Resolution Imaging Spectroradiometer (MODIS) data, *Kaufman et al.* [2005a, 2005b] separated aerosols into three quasi-independent classes: maritime sea salt (SS), dust (DU), and anthropogenic (AN) aerosols based on MODIS retrieved AOT and FMF data. In this classification, the SS and DU are categorized as "natural" although a fraction of DU could be due to human activity. This methodology classifies "anthropogenic" aerosols as those that have a large small-mode AOT contribution. Here, we define anthropogenic as those aerosols likely to be produced from human activity, which are primarily made up of sulfates (SU), organic carbon (OC), and black carbon (BC). Naturally occurring OC and SU can also contribute to small-mode AOT, but the contribution is generally small.

[4] To classify aerosol type, *Kaufman et al.* [2005a, 2005b] use the ratio of small mode AOT to the total AOT at 0.55 μm that is called the fine mode fraction (FMF). Anthropogenic AOT is dominated by small-mode ($0.1 < r_e < 0.25$ μm) aerosols while naturally occurring aerosols in the form of DU and SS are dominated by coarse-mode aerosols ($1.0 < r_e < 2.5$ μm) where r_e denotes aerosol effective radius [*Kaufman et al.*, 2001; *Tanre et al.*, 2001]. Both small-mode and coarse-mode AOT over the ocean are retrieved from MODIS radiances using a combination of 4 small-mode ($r_e < 1.0$ μm) and 5 coarse-mode ($r_e > 1.0$ μm) aerosol models with the relative amounts of small-mode to coarse-mode aerosols adjusted until a solution is found which minimizes error in the observed radiance [*Remer et al.*, 2005]. Small aerosol particles, such as those produced from anthropogenic (AN) sources predominantly have higher FMF values, while naturally occurring DU and SS aerosols with larger particles have predominantly smaller FMF values [e.g., *Bellouin et al.*, 2005]. Using Aerosol Robotic Network (AERONET), and later MODIS AOT of selected regions associated with primarily SS, DU, or AN aerosols, *Kaufman et al.* [2005a, 2005b] derived FMF values for each aerosol type (Table 1). Using AERONET and aircraft data over selected regions, *Bellouin et al.* [2005] also derived FMF values for AN, DU and SS aerosols. The FMF values for AN aerosols reported by *Bellouin et al.* [2005] are lower that those reported by *Kaufman et al.* [2005a, 2005b].

[5] Uncertainty up to 30% exists with MODIS FMF values over the ocean [*Kaufman et al.*, 2005a; *Kleidman et al.*, 2005]. Uncertainty is generally higher for naturally occurring aerosols [*Bellouin et al.*, 2005; *Kaufman et al.*, 2005a] especially SS, as seen by the large standard deviations (Table 1). *Christopher et al.* [2006] and *Christopher and Jones* [2007] have applied these FMF values to global and regional domains respectively using the assumption that the FMF for each aerosol type does not vary as a function of space and time. The implications of this assumption can be illustrated by applying a random perturbation to the *Kaufman et al.* [2005a, 2005b] FMF thresholds when calculating the DU component of AOT over 500 simulations. The perturbations are bounded using the uncertainly values (standard deviations) for each aerosol type given by *Kaufman et al.* [2005a] and also Table 1. As an example, using the methods described by *Christopher and Jones* [2007], DU AOT was used to derive the global mean cloud-free shortwave radiative effect (SWRE) at the top of atmosphere (TOA) for DU aerosols for each random perturbation. The uncertainties for SS, DU, and AN FMF listed in Table 1 result in a ±25% change from the mean dust SWRE, and this does not take into account the additional uncertainties present in the data such as cloud contamination and angular dependence models [*Christopher et al.*, 2006]. Anthropogenic forcing is not as sensitive to variations in FMF thresholds, with only a ±15% change observed indicating that the MODIS FMF are useful for calculating AN aerosol radiative forcing.

[6] In this study, we assess several satellite observable parameters of SS, DU, and AN in greater detail to examine these uncertainties and to determine their spatial and temporal variability relative aerosol species. To accomplish this, we combined multiple-satellite data sets from the MODIS, Total Ozone Mapping Spectrometer (TOMS), and Measurements of Pollution in the Troposphere (MOPITT) with modeling results from the Goddard Global Ozone Chemistry Aerosol Radiation Transport (GOCART) [*Chin et al.*, 2004] to define and examine regions dominated by one of the three (SS, DU, AN) major aerosol species. The sensitivities of each instrument (and model) to differing aerosol types are summarized in Table 2. MODIS, TOMS, and MOPITT data are all independent of one another and are used to describe aerosol species whose spatial and temporal distribution is defined using GOCART.

[7] In addition to separating total AOT into broad SS, DU, and AN components, GOCART further separates AN aerosols into black carbon (BC), organic carbon (OC), and sulfate (SU) components from anthropogenic sources only. The light absorbing BC is primarily due to incomplete combustion of fossil and biomass fuels whereas OC is directly produced by combustion sources or gas to particle conversion [*Reid et al.*, 2005]. Sulfate on the other hand is primarily from the oxidation of sulfur dioxide produced in the combustion of fossil fuels in the industrial and power sectors [*Koch et al.*, 2007].

Table 2. Sensitivity of Different Satellite-Based Sensors (MODIS, TOMS, and MOPITT) to Different Aerosol Species[a]

Sensor	SS	DU	AN	PO	BB
MODIS	yes	yes	yes		
TOMS-AI		yes	yes[b]		yes
MOPITT-CO			yes[c]		yes
GOCART	yes	yes	yes	yes	yes

[a]"Yes" indicates that data from this sensor can be useful at discriminating between individual aerosol species. GOCART models each of these aerosol species separately and is used to define regions where one is predominate over the others. Observed aerosol properties in these regions are then calculated.
[b]Absorbing aerosols above the boundary layer.
[c]Tracer for carbonate aerosols.

[8] Within each GOCART defined aerosol species region, the MODIS AOT and FMF, along with TOMS-AI and MOPITT CO data, are analyzed to determine the observed properties of each aerosol species. These observations are then used to derive monthly statistics describing SS, DU, and AN as a function of space and time. The use of GOCART to constrain aerosol species regions also allows us to contrast the properties of AN aerosols produced from biomass burning (BB), which are high in BC and OC versus those produced from pollution (PO). Pollution-type aerosols, in general, contain high concentrations of SU, compared to carbonates that are more prevalent in biomass and residential combustion. However, it is important to note that while SU is the dominant anthropogenic aerosol type in south Asia, carbonates (both OC and BC) remain a significant contributor to the anthropogenic component of AOT [*Koch et al.*, 2007]. The combined model and satellite based analysis will help better quantify the different characteristics of various aerosol species, which is necessary for future research involving radiative effect as a function of aerosol type.

2. Data

2.1. Moderate Resolution Imaging Spectroradiometer (MODIS)

[9] Total and small-mode 0.55 μm AOT data from the MODIS instrument aboard the Terra satellite are obtained over the global oceans only from the MOD04, Collection 5 aerosol product [*Remer et al.*, 2006] with a spatial resolution of 10 km at nadir. MODIS data are acquired for the period between December 2003 and November 2004. A previous iteration of this research used data from 2001, but FMF data between October 2000 and June 2001 were found to be unreliable because of the switch from Side A to Side B electronics [*Chu et al.*, 2005]. We are primarily concerned with aerosol speciation in clear-sky regions, with changes in aerosol size parameters in the vicinity of clouds considered beyond the scope of this work. While MODIS AOT retrieves are only made for the clear-sky portion of a 10 km pixel, mostly cloudy pixels may result in unrepresentative AOT values [*Zhang and Reid*, 2006]. To reduce this effect, we chose to remove all pixels with a MODIS cloud fraction greater than 30%, a threshold that was shown by P. Gupta and S. A. Christopher (Long term particulate matter trends derived using surface and satellite measurements, submitted to *Atmospheric Environment,* 2007) to provide a balance between eliminating too many pixels with a stricter cloud fraction threshold and including too many pixels with a higher cloud fraction AOT data. Both "marginal" and "best" retrievals are used, as eliminating marginal removes almost 90% of the possible data points, many of which happen to be small-mode aerosols. As a result, using only best retrievals would bias the results toward larger aerosol types.

[10] We are primarily concerned with over-ocean aerosol characteristics only since small mode AOT retrievals over land surfaces have much larger uncertainties [*Remer and Kaufman*, 2005]. Over the ocean, the uncertainty of AOT can be expressed as $\varepsilon = 0.03 \pm 0.05\tau$, with FMF uncertainty on the order of 30%. The complete retrieval algorithm, the uncertainties and intercomparisons with the AERONET are provided by *Remer et al.* [2005]. This research is primarily concerned with quantifying the differences in aerosol properties as observed from satellite, and as a result should not be sensitive to biases in the data compared to other ground or aircraft based measurements (e.g., AERONET).

2.2. TOMS Aerosol Index (AI)

[11] The Total Ozone Mapping Spectrometer (TOMS) aboard the NASA Earth Probe satellite, which has a 1030 local time descending equatorial crossing time was originally designed to study global ozone concentration, but can also be used to study aerosol concentration and type [*Hsu et al.*, 2000]. In particular, DU and BB aerosols absorb radiation at UV wavelengths when compared to a clear-sky or even a maritime aerosol background [*Torres et al.*, 2002]. Highly absorbing carbonaceous and DU aerosols above the boundary layer are most sensitive to UV radiation. TOMS AI is less sensitive AN aerosols resulting from pollution, which contain a high proportion of SU. In general, AI is not sensitive to either aerosol types below the boundary layer (H < 1 km). The relationship between UV radiation and absorbing aerosol concentration is defined in terms of the TOMS aerosol index (AI), which is the difference between the UV observations and model calculations from a pure molecular atmosphere with the same surface and measurement conditions. Positive values for AI indicates the presence of UV-absorbing DU or BB aerosols in the mid and upper troposphere, while near zero and negative values are indicative of nonabsorbing, small-mode, and/or aerosols near the surface. For this study, daily mean level 3 TOMS AI data at 1 $\times$ 1 degree grids were acquired for the 2003–2004 study period and were used to calculate regional means and to examine monthly variations absorbing aerosols. It should be noted that the level 3 product sets negative AI values equal to zero, which results in an overestimation (positive bias) of AI when mostly nonabsorbing aerosols (e.g., sea salt) are present.

2.3. Goddard Chemistry Aerosol Radiation Transport (GOCART)

[12] The satellite observed AOT properties are compared with AOT simulations produced by the GOCART model [*Chin et al.*, 2004]. The GOCART simulates the transport of aerosols and their type over a global domain. Aerosols are categorized as BC, OC, SU, DU and SS. Monthly averaged data on a 2.5 $\times$ 2 degree grid were acquired for each region between December 2003 and November 2004. FMF from

GOCART is the ratio of the sum of the optical depth from SU, OC, BC, submicron DU and SS to the total AOT while AN aerosols are defined as the sum of BC, OC and SU from anthropogenic sources only. *Chin* [2002] and *Chin et al.* [2004] provide a thorough description of the differences between the MODIS and GOCART. GOCART uses global emissions of aerosols and assimilated meteorological fields to calculate the mass loading of each aerosol species separately that are then converted to AOT using mass extinction coefficients.

[13] Over oceans, the MODIS is limited to areas without clouds and sunglint whereas the GOCART calculates AOT in clear, cloudy, and sunglint conditions. Because of these differences between the GOCART and MODIS, differing AOT values are always to be expected. By comparison, the MODIS does not obtain AOTs for specific aerosol components but it uses the FMF as a surrogate for identifying broad aerosol types [*Kaufman et al.*, 2005a, 2005b]. Note that the goal of our study is not to assess the difference between the absolute magnitudes of the AOT or the FMF from GOCART and MODIS. Rather, we use the GOCART output to assess the distribution of SS, DU and AN AOTs over a particular area to define regions composed of primarily a single aerosol species. Observed aerosol properties are then derived for regions where a single aerosol type is expected according to GOCART.

2.4. Measurement of Pollution in the Troposphere (MOPITT)

[14] The MOPITT instrument on the Terra satellite measures atmospheric carbon monoxide (CO) concentrations [*Edwards et al.*, 2004]. MOPITT is an infrared gas correlation radiometer that retrieves the vertical profile of CO at 7 levels (surface to 150 hPa) with a nadir resolution of 22 km [*Deeter et al.*, 2003]. MOPITT is most sensitive to CO in the midlevels (700–500 hPa) of the atmosphere with information from multiple infrared bands used to derive CO concentrations and other levels. Since the dominant sources of CO are related to the carbon emissions of biomass and fossil fuel burning, the CO signature should also be highly correlated with the anthropogenic component of AOT [*Bremer et al.*, 2004; *Edwards et al.*, 2004]. However, it is important to note that the CO lifetime in the troposphere is about 2 months whereas aerosols have a much shorter life time, on the order of days to a week. The MOPITT is not as sensitive to boundary layer CO whereas the MODIS AOT is sensitive to boundary layer aerosols. Since CO is directly related to carbon emissions and less so for sulfate, MOPITT data between BB and PO regions are compared to determine if significant differences exist in CO observations between these regions (and compared to all AN aerosols) and provide an insight into their vertical distribution. We use the daily mean version 3, level 3 data product that is interpolated to a uniform 1×1 degree grid. The estimated uncertainty of CO profiles within the level 3 product is within ±15% of observed values [*Edwards et al.*, 2004].

2.5. NCEP Reanalysis

[15] Monthly mean, global surface wind speed and direction, and humidity data were obtained from National Centers for Environmental Prediction (NCEP) Reanalysis data. The NCEP Reanalysis contains global meteorological conditions with a 2.5 degree horizontal resolution and a 17 level vertical resolution at 6 hour time intervals [*Kalnay et al.*, 1996]. The reanalysis data set reliability captures synoptic-scale dynamic and thermodynamic features, though often misses smaller-scale phenomena. The wind speed and direction fields have been shown to be quite accurate; however, a dry bias in the low-level and midlevel humidity (<5 km) fields does exist. Since we are only concerned with monthly averages and changes in thermodynamic fields, these issues are not a major concern of this research.

3. Methodology

[16] Global MODIS, TOMS-AI, GOCART, and MOPITT data are placed into a common, monthly mean 2×2 degree grid for comparison by averaging all available data within a specific 2×2 degree grid cell. GOCART data is only available as a monthly mean product with a coarse spatial resolution and as a result, the use of a higher-resolution grid for other satellite data sets would not increase the quality of this research. Regions composed primarily of SS, DU, or AN aerosols are defined as areas where at least 80% of the total GOCART AOT is composed of a single aerosol type. Higher thresholds, which would reduce uncertainty, resulted in smaller number of pixels for individual aerosol-type regions that were too small for analysis. Using 80% allows for sufficiently large spatial coverage of each aerosol species on a month by month basis to then calculate the satellite observed characteristics of that aerosol. It is important to note that the spatial extent and location of aerosol specific regions are not predefined and are allowed to change as aerosol characteristics change during the course of the year. As a result, it is possible to track the movement and change in spatial extent of various aerosol species regions.

[17] GOCART defines AN as small-mode aerosols resulting from human induced sources only. The contributions to small-mode from natural sources, such as DMS, are not considered as part of the anthropogenic AOT component. The resulting FMF, TOMS-AI, and MOPITT CO values for GOCART defined AN regions will therefore only represent the observable characteristics of anthropogenic sources of small-mode AOT. The AN regions are further subdivided into PO and BB aerosol types. In this research the former primarily includes the Indian Ocean and western Pacific regions north of the equator, while the latter is primarily located in the central Atlantic Ocean off the west coast of Africa. The concentration of BB aerosols is highly seasonal and is maximized during the dry season between August-October in the eastern Atlantic. To separate BB and PO aerosols, GOCART modeled BC, OC, and SU components of anthropogenic AOT are utilized. PO regions are defined where the sulfate proportion of the anthropogenic AOT exceeds 70%. BB regions are defined when the anthropogenic AOT is composed of at least 70% OC + BC. We use a 70% threshold here since carbonates or sulfates alone rarely account for more than 80% of the total anthropogenic AOT. As a result, we accept that a greater uncertainty exists in PO versus BB comparisons. For some months, regions containing primarily a single aerosol type or subtype may not be large enough to produce

significant results. For these cases, no numerical satellite derived statistics are reported.

[18] In order to derive satellite observed properties representative of each aerosol species, the MODIS, TOMS, and MOPITT data within each specific aerosol region defined using the GOCART data must be extracted. From these data, mean and standard deviation statistics are computed for each sensor. Probability density functions (PDFs) of FMF for each aerosol type are created from the raw daily data. Since the 80% threshold is used to determine individual aerosol species regions, up to 20% of the total AOT is made up of minor aerosol species. To reduce the influence of minor aerosol types when deriving FMF properties for each aerosol types, it is advantageous to remove FMF values that are likely associated with the minor aerosol species that make up the remainder of the AOT. To accomplish this, cumulative histograms for FMF are computed for each aerosol species and the 20% of SS and AN FMF distributions least likely to be associated with that aerosol species are removed.

[19] For AN aerosols, MODIS FMF values are removed if they occur below the value corresponding to the 20% cumulative probability of AN FMF within each region. We make the assumption on the basis of previously observed characteristics of SS, DU, and AN aerosols that many of the coarse mode aerosols observed in AN regions are a reflection of the SS background, having much smaller FMF than most anthropogenic aerosols [*Bellouin et al.*, 2005; *Kaufman et al.*, 2005a, 2005b]. We recognize that we may be removing some coarse mode anthropogenic aerosols, but that is compensated by the notion that some small mode SS and DU remain. For SS, data are removed if FMF is greater than the 80% cumulative probability threshold. Dust is treated somewhat differently whereby the upper and lower 10% of FMF values are removed prior to averaging. After excluding these values, the average FMF value is calculated for each aerosol type region and month where sufficient data are available.

4. Results

4.1. Regional Overview

[20] Regions dominated by a single aerosol type are not static and change substantially in spatial extent over time. Figure 1 shows the spatial extent of aerosols where at least 80% of the total AOT is composed of either SS, DU, or AN components as defined by the GOCART between January and November 2004. Regions consisting primarily of a single aerosol species account for approximately 25% of the atmosphere over the global oceans. The remaining areas are considered a mix of aerosol types. With the exception of the northern Indian Ocean, these areas generally have low overall AOTs with SS accounting for a large, but not quite dominant, portion of the total AOT. In the northern Indian Ocean, high AOTs during the summer months are associated with a mix of mineral dust and anthropogenic aerosols [*Ramana and Ramanathan*, 2006]. For illustration purposes, data from every other month are shown. During January (Figure 1a), DU is confined to a narrow strip over the Atlantic Ocean west of the West African coast, since the prevailing wind patterns in this region are not favorable for transport of DU into the central Atlantic. AN aerosols are located in the Arabian Sea and Bay of Bengal with a secondary concentration being present in the Gulf of Mexico. Both regions contain a large proportion of PO based aerosols as evidenced by the shaded regions where the AN AOT is at least 70% from SU-type aerosols. The BB region is confined to a very small area over the Atlantic northwest of Angola.

[21] Between March and May, the concentration of AN decreases in the Gulf of Mexico region, with the exception of locations in close proximity to Mexico City (Figures 1b and 1c). The AN aerosol concentration in the Arabian Sea slowly decreases because of the influx of DU aerosols, while AN concentration increases in regions off southeast Asia such as the South China Sea. The onset of the BB season in southern Africa is noticeable with a large increase in the AN region west of Angola between March and May. However, the presence of a significant SU concentration prevented them from being classified as primarily BB at this time. DU areas are also increased compared to January and February owing to greater transport of dust aerosols into the Atlantic.

[22] During July (Figure 1d), AN regions are most prevalent over the ocean west of central Africa, in association with an increase in BB [*Myhre et al.*, 2004]. Small regions of PO aerosols exist off the eastern United States and Indonesia. The latter area increases in spatial extent significantly during August and September (Figure 1e). DU over the Atlantic is also maximized during the Northern Hemisphere summer [*Prospero et al.*, 2002; *Kaufman et al.*, 2005b]. By September, DU aerosol coverage in the eastern Atlantic begins to decrease; however, BB aerosol originating from Africa and now the Amazon in South America still populate large regions of the south Atlantic and far eastern Pacific (Figure 1e). By November, with the monsoon season over, DU is also no longer being transported into the Indian Ocean and the primary contributor to AOT is again PO (Figure 1f). During all times of the year, regions dominated by SS are associated with regions with high mean wind speeds that do not correspond with any overland aerosol source region. As a result, the SS regions are generally confined to the large open ocean basins of the Southern Hemisphere. Interestingly, the areal coverage of SS aerosols decreases during the course of the year, and may be a result of GOCART underestimating AOT from sea-salt aerosols under certain conditions.

[23] Given this wide variety of aerosol types in differing regions, it cannot be expected that the observed characteristics of generic aerosol types (SS, DU, AN) would be the same for each region and time given the differing source regions of certain aerosols. This is especially true for various species of AN aerosols, which include both PO and BB. Since various satellite-based instruments are sensitive to the differing properties between PO and BB aerosols (Table 2), data from these sensors should be able to unambiguously distinguish one aerosol species from another. To test this hypothesis, MODIS FMF, TOMS-AI, and MOPITT CO characteristics are compiled for each aerosol species on a monthly basis, with AN regions further split into BB and PO aerosols. It will be shown below that each aerosol species has unique satellite observable charac-

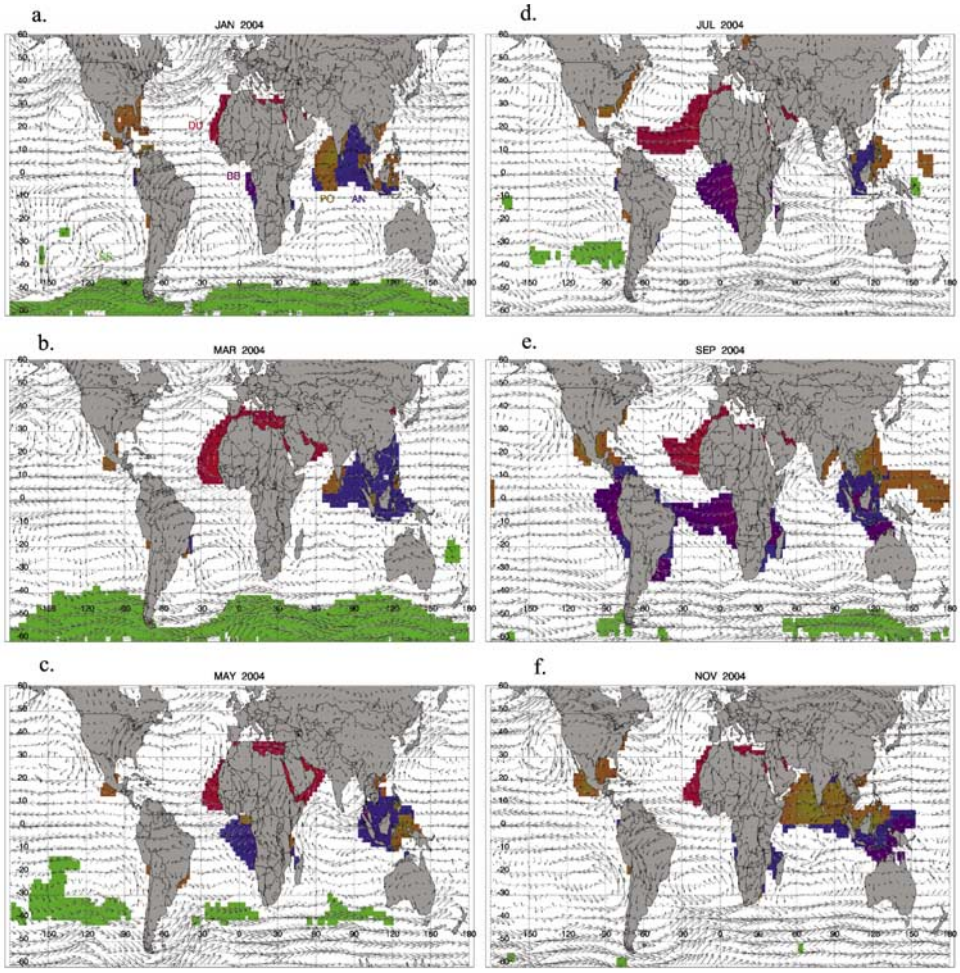

Figure 1. Regions where at least 80% of total GOCART AOT is a result of a single aerosol type (SS (green), DU (red), or AN (blue)). Anthropogenic aerosols are further subdivided into predominately (>70%) BB (purple) and PO (brown) regions. Vectors represent 850 hPa (black) and 700 hPa (gray) wind speed and direction during each month and are derived from 2.5° resolution NCEP Reanalysis. Monthly averaged aerosol components are for (a) January, (b) March, (c) May, (d) July, (e) September, and (f) November 2004 respectively.

teristics, but that those characteristics often change during the course of the year.

4.2. MODIS and TOMS-AI Aerosol Species Characteristics

[24] The total MODIS AOT does not vary substantially on a monthly basis, with only minor increases during the spring months (Table 3). GOCART derived AOTs are similar to those reported by MODIS, but with a slightly larger monthly variation, consistent with results reported by *Chin et al.* [2004]. Globally averaged MODIS FMF remains relatively constant (0.53 ± 0.02) during the 12 month study period, but FMF associated with specific aerosol types do show some seasonal variability (Figure 2). A clear separation generally exists in monthly averaged FMF for SS, DU, and AN aerosols (Figure 2). The most significant exception occurs during December and January when both SS and DU have FMF averages near 0.4 (Table 1).

[25] AN aerosols are primarily located in the Indian Ocean and South China Sea regions between December 2003 and April 2004. These aerosols are primarily as result of PO aerosols transported southward. During this period, anthropogenic FMF values range between 0.82 and 0.87 with a corresponding r_e of only 0.3 μm (Table 3 and Figures 2 and 3a). FMF for AN aerosols decreases by ~15% during June compared to the remainder of the year (Figure 2). A corresponding increase in MODIS retrieved aerosol r_e was also observed during this time (Figure 3a). Several possibilities exist as to why FMF decreases and r_e increase in June. First, it may just be a sampling artifact occurring with the June data. However, the magnitude of the drop and the lack of any noticeable changes in sampling characteristics between June and other months suggests other factors are responsible. In the Indian Ocean and surrounding area, and increase in the mean low-level to midlevel relative humidity was observed during this period, which could act in increase the size of hygroscopic aerosols, especially PO. Another is the possibility that DU that acquire an anthropogenic coating are being classified as AN by GOCART.

Table 3. Monthly Averaged GOCART (GO) AOT, MODIS AOT, and MODIS FMF Over a Global Domain (Surface Area Weighted) Between December 2003 and November 2004[a]

Month	GO AOT	MOD AOT	FMF	SS	DU	AN	PO	BB
12	0.10	0.12	0.52	0.44 ± 0.09	0.42 ± 0.05	0.84 ± 0.05	0.84 ± 0.05	0.84 ± 0.04
1	0.09	0.11	0.56	0.40 ± 0.09	0.44 ± 0.06	0.82 ± 0.06	0.81 ± 0.06	NA
2	0.11	0.13	0.53	0.27 ± 0.07	0.48 ± 0.05	0.84 ± 0.06	0.82 ± 0.05	NA
3	0.13	0.15	0.50	0.19 ± 0.04	0.52 ± 0.11	0.87 ± 0.04	0.85 ± 0.05	NA
4	0.13	0.13	0.51	0.24 ± 0.06	0.46 ± 0.09	0.86 ± 0.04	0.87 ± 0.05	NA
5	0.15	0.13	0.53	0.23 ± 0.06	0.38 ± 0.06	0.83 ± 0.06	0.84 ± 0.06	NA
6	0.14	0.14	0.51	0.27 ± 0.06	0.38 ± 0.06	0.74 ± 0.08	0.72 ± 0.08	NA
7	0.11	0.13	0.55	0.24 ± 0.09	0.34 ± 0.04	0.80 ± 0.09	0.85 ± 0.06	0.75 ± 0.09
8	0.11	0.12	0.53	0.18 ± 0.05	0.40 ± 0.06	0.85 ± 0.07	0.88 ± 0.04	0.84 ± 0.08
9	0.11	0.12	0.52	0.15 ± 0.04	0.44 ± 0.08	0.83 ± 0.07	0.84 ± 0.06	0.82 ± 0.08
10	0.11	0.13	0.53	0.16 ± 0.04	0.51 ± 0.06	0.86 ± 0.05	0.85 ± 0.05	0.86 ± 0.04
11	0.10	0.11	0.55	NA	0.49 ± 0.05	0.85 ± 0.06	0.83 ± 0.06	0.89 ± 0.04

[a]Average MODIS FMF values for sea salt (SS), dust (DU), total anthropogenic (AN), biomass burning (BB), and pollution (PO) regions are also listed where sufficient data exist.

[26] Dust aerosols are generally confined to the region west of the Saharan Desert in the North Atlantic Ocean, and transported into the North Atlantic primarily on the basis of wind speed and direction (Figure 1). Dust FMF values range between 0.34 and 0.52 with an overall mean of 0.44 ± 0.06, somewhat below that given by *Kaufman et al.* [2005a, 2005b] (Table 1 and Figure 2). A decrease in DU FMF was also observed during the summer months (JJA) compared to the spring and fall seasons corresponding to a small increase in MODIS r_e during these same months (Figures 2 and 3a). However, the reason for this decrease remains unclear. This may be a simple reflection of larger dust particles being transported over the ocean to do stronger easterly winds. Differences in modeled versus observed DU and AN aerosols may also play a factor. Further research is necessary to resolve the cause of the seasonality in DU and AN aerosol size.

[27] Dust aerosols can also be identified using TOMS-AI, owing to the UV absorbing nature of atmospheric mineral DU compared to either SS or AN aerosols, which are generally nonabsorbing (with the exception of BB). Between April and September, when DU transport from the Saharan Desert over the North Atlantic is maximized, TOMS-AI for DU regions is consistently higher than either AN or SS values despite the latter's likely overestimation due to the lack of negative AI values in the level 3 data (Figure 4). Between May and July, when mineral dust is maximized in the Atlantic, monthly TOMS-AI values of dust are well separated from both AN and especially SS values. Vertical profiles of dust AOT produced by GOCART also indicate the presence of dust aerosols in the mid and even upper troposphere, also contributing to the high TOMS-AI values observed. During other months, TOMS-AI values for all three primary aerosol species generally remain low (<1.0). While DU is present during this time, the concentration is much lower, and it is not being transported as high into the atmosphere, making it harder to resolve with AI [*Kaufman et al.*, 2005a].

[28] SS FMF values show the greatest variability as a function of time, due to an apparent drop in FMF from ~0.4 to ~0.2 (and a corresponding increase in r_e) between December and March (Figure 2). Overall uncertainty for SS is greatest with monthly standard deviations sometimes exceeding 25% of the mean value. Regions containing primarily SS aerosols consistently have higher wind speeds than DU and AN regions as would be expected since SS AOT should be greatest in the presence of strong winds (Figure 3b). However, no significant correlation between FMF values in predominately SS regions and surface wind speed was observed. (For other aerosol species, the wind speed and direction is important to transport of land-based aerosols over oceanic regions). It is possible that the substantial decrease in the areal coverage of predominately SS aerosols after June is a result of unrepresentative samples during this part of the year. In fact, the SS region was so small for November, that no SS statistics could be derived. GOCART has a tendency to underestimate the maritime component of AOT and even a small concentration of another aerosol species would be enough to account for more than 20% of the total AOT. A slight increase in modeled DMS was observed during this time, but it is not known if this is real or a model artifact. In any event, SS FMF values are consistently smaller than those for either

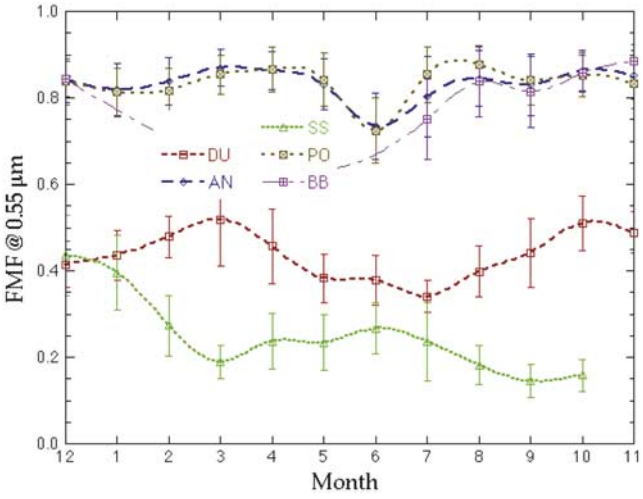

Figure 2. Time series from December 2003 to November 2004 of monthly averaged FMF values for each aerosol specific region, defined using GOCART data. The smallest FMF values correspond to sea salt, with dust next, and finally anthropogenic aerosols having the largest FMF.

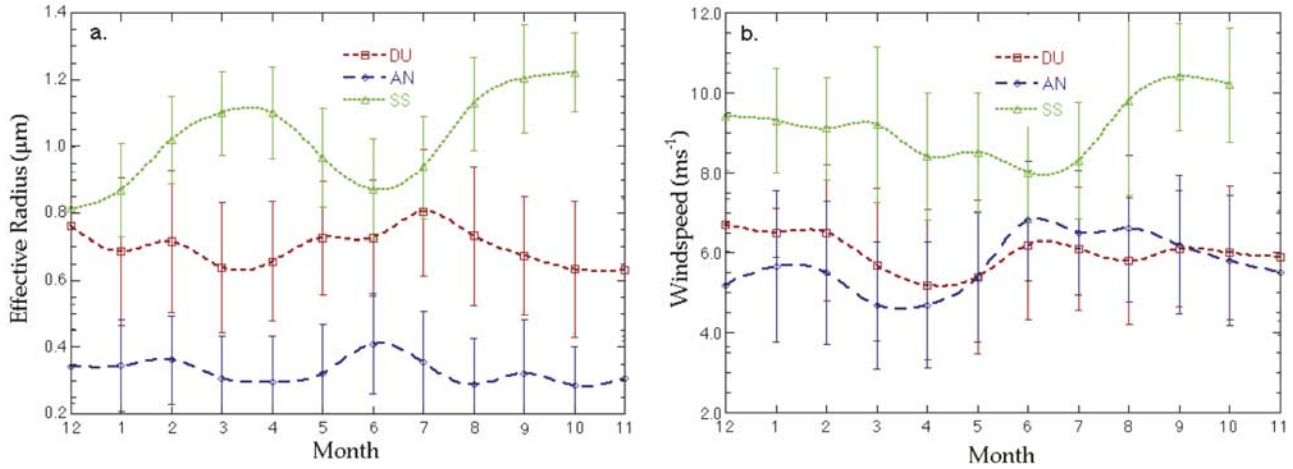

Figure 3. Time series of monthly averaged MODIS (a) effective radius and (b) near-surface wind speed for SS, DU, and AN aerosol species.

DU or AN aerosols, which is consistent with *Kaufman et al.* [2005a].

[29] Yearly averaged FMF values for SS, DU, and AN based on our analysis are 0.25 ± 0.09, 0.44 ± 0.06, and 0.83 ± 0.04, which are in general agreement with previous research (Table 1). The overall FMF values reported here agrees well with those reported from AERONET/aircraft data in the work by *Bellouin et al.* [2005], but are generally lower than those reported by *Kaufman et al.* [2005a, 2005b]. However, the differences either fall within or near the uncertainty limits (standard deviations) presented by both studies. Given the highly variable nature of FMF as a function of space, time, and aerosol characteristics (within broad aerosol types), further reduction in ''uncertainty'' may not be possible using satellite data and numerical modeling simulations alone and may require detailed analysis of in situ data. The natural variability of these aerosols must be recognized, and only spatially and temporally appropriate values used in future research.

4.3. Biomass Burning (BB) Versus Pollution (PO)

[30] During the winter months (NDJF), aerosols originating from PO aerosols in the northern Indian Ocean are the primary contributor to the AN component of AOT. In central Africa as BB increases during April and May, these aerosols are transported westward over the Atlantic Ocean resulting in a large area of AN aerosols in the south Atlantic. Both carbonates and SU are large contributors, but the concentration and areal coverage of carbonates increases substantially between May and July (Figures 1c and 1d). The size of the BB regions increases until September at which point it stretches across the Atlantic into South America, with additional BB aerosols being transported westward from BB on that content as well (Figure 1e). The increased influence of BB can be seen using the GOCART modeled BC, OC, and SU concentrations for AN regions only. During the months when PO is more dominant (NDJF), SU accounts for approximately 65% of the anthropogenic AOT (Figure 5). The contribution from SU decreases to near 55% between August and November corresponding to the maxima of south African biomass burning. As a result, the OC portion of the anthropogenic AOT increases from 20% to near 35% during this period. The contribution from BC remains approximately constant between 10 and 13%.

[31] Given the change in AN aerosol species modeled by GOCART, we assess the characteristics of BB and PO aerosols using MODIS and TOMS-AI observations. Significant regions of both BB and PO aerosols only exist on a continuous basis between July and November; thus the comparison between these aerosol types is limited to this 5 month period. For this period, no consistent or significant differences between PO and BB monthly FMF averages were observed (Figure 2). However, TOMS-AI observations showed a much more significant difference between BB and PO aerosols with AI for BB being up to 50% greater than corresponding values for PO during this period (Figure 4). This is a result of the TOMS instrument's greater sensitivity to absorbing aerosols (carbonates) that located higher in the atmosphere. Evidence that BB aerosols are present at higher levels is derived from GOCART output. In BB regions, GOCART AOT is maximized at higher levels than corresponding PO AOT, indicating that BB aerosols are present at higher levels. However, the variability of TOMS-

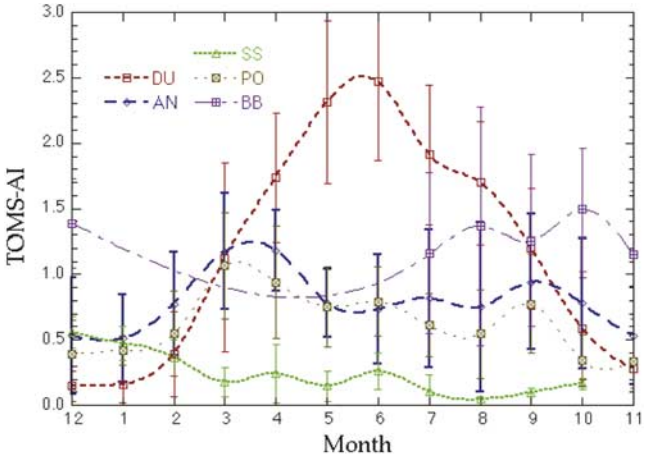

Figure 4. Same as Figure 2 but for monthly averaged level 3 TOMS-AI for each aerosol species.

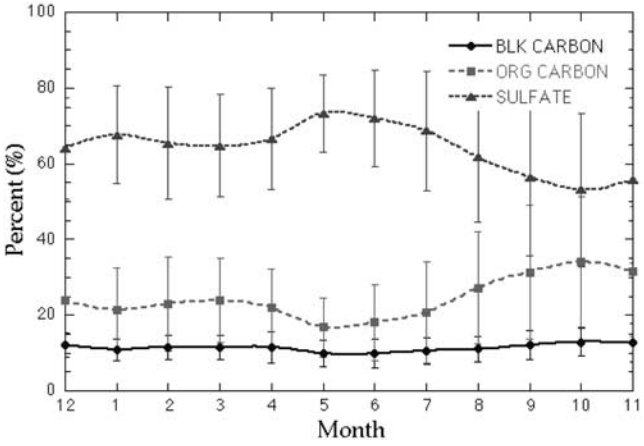

Figure 5. Proportion (%) of monthly mean anthropogenic AOT, defined by GOCART, from black carbon (BC), organic carbon (OC), and sulfate (SU) aerosols. Note that OC increases between June and September at the expense of SU.

AI in BB regions is quite large, never quite being independent (by one or more standard deviations) of TOMS-AI in PO regions.

[32] Another product available for separating BB from PO is carbon monoxide (CO) data from the MOPITT instrument. CO acts as a tracer gas for some aerosol species, especially those produced from biomass burning [*Edwards et al.*, 2004]. As a result, CO values resulting from BB should exceed those from PO regions. Between July and October when the transport of BB over the Atlantic is greatest, total column CO is higher for BB compared to PO regions, though both have large monthly variability (Figure 6a). Analysis of the vertical distribution of CO during September in AN regions only indicates that BB is distributed throughout much of the troposphere with CO values for BB regions exceeding PO values by a significant margin up to the 500 hPa level, and possibly up to even 250 hPa (Figure 6b). The differences between TOMS-AI and MOPITT CO values observed for BB and PO regions indicates that these sensors, in combination with MODIS AOT and FMF data, provide a powerful tool for future research involving the quantitative separation of aerosol types on a global scale.

5. Summary and Conclusions

[33] The results of this research indicate that various aerosol species constrained using GOCART model output do indeed display unique characteristics when observed from various satellite remote sensing platforms. MODIS AOT, FMF, and r_e measurements resolve aerosol size quite well, making it possible to produce defining characteristics for aerosol species such as SS, DU, and AN. As expected, aerosol size generally increases from anthropogenic, through dust, and finally maritime aerosols. This corresponds to large FMF values for anthropogenic aerosols and smaller FMF values for DU and SS. The FMF values reported here for each type correspond well with those presented by *Bellouin et al.* [2005], but are somewhat lower than those reported by *Kaufman et al.* [2005a, 2005b]. However, FMF and r_e statistics for each aerosol type change as a function of space and time making the use of a single defining FMF value problematic. Additional aerosol properties were defined using TOMS-AI measurements, which is sensitive to UV absorbing aerosols such as BB and mineral dust and the height of those aerosols in the atmosphere. Dust aerosols, which are generally large in size and present in the midlevels of the atmosphere generally had much higher TOMS-AI values than either AN or SS aerosols during the summer months.

[34] The difference between MODIS FMF for the BB and PO components of anthropogenic AOT was quite small. However, TOMS-AI as well as MOPITT CO values between the GOCART defined BB and PO regions differs substantially. For both AI and CO, values associated with BB regions were higher than corresponding sulfate dominated PO regions. Unfortunately, the lack of large BB regions limited this portion of the analysis to the 5 month period between July and November. In other years, such as

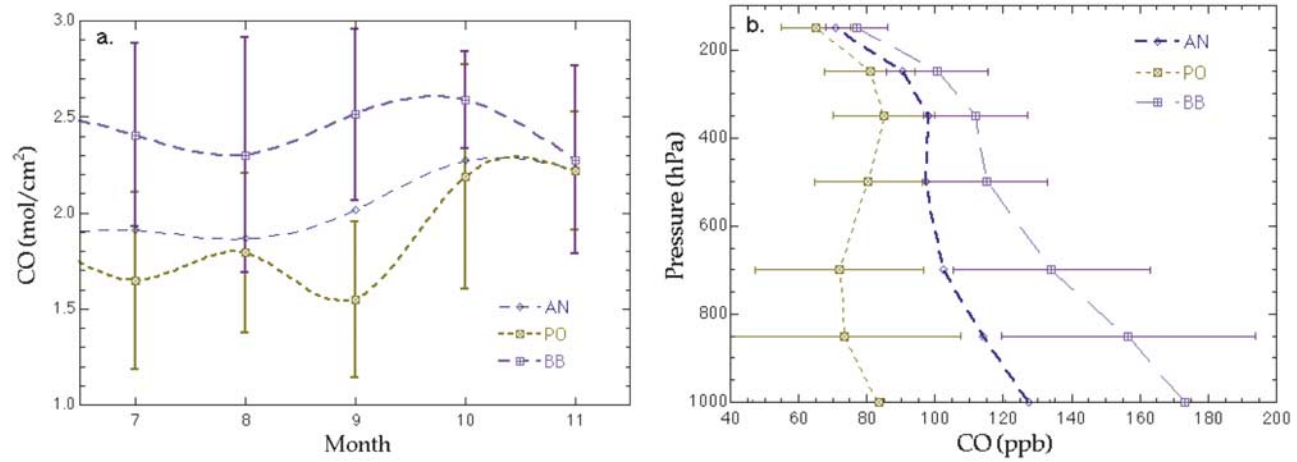

Figure 6. (a) Times series from May to November 2004 of total column MOPITT CO for the BB, PO, and total AN regions. (b) Total column CO values are given in units of 10^{18} mol/cm^2. Vertical distribution of MOPITT CO for BB, PO, and total AN aerosol for September 2004.

2001, a secondary biomass burning region was observed in April surrounding Central America. Preliminary analysis indicates that these aerosols had somewhat different characteristics than those produced from African biomass burning. The combination of GOCART modeled aerosol species with observations from multiple satellite observing platforms as allowed the production for the first time, a listing of distinguishing statistics for various aerosol types. Future research will add additional in situ data sources that will be helpful in determining the effect of aerosol type on SW radiative effect.

[35] **Acknowledgments.** This research was supported by NASA's Radiation sciences, Interdisciplinary sciences, an EOS grant, and ACMAP programs. The CERES SSF data that contain the merged MODIS and CERES and the MOPITT data were obtained through the NASA Langley Distributed Active Archive Systems. The MODIS daily products were obtained from the Goddard Distributed Active Archive Systems. Special thanks to Mian Chin for providing the GOCART results. We graciously appreciate the rigorous reviews that helped improve the overall quality of the manuscript.

References

Bellouin, N., O. Boucher, J. Haywood, and M. S. Reddy (2005), Global estimate of aerosol direct radiative forcing from satellite measurements, *Nature*, *438*, 1138–1141, doi:10.1038/nature04348.

Bremer, H., et al. (2004), Spatial and temporal variation of MOPITT CO in Africa and South America: A comparison with SHADOZ ozone and MODIS aerosol, *J. Geophys. Res.*, *109*, D12304, doi:10.1029/2003JD004234.

Chin, M. (2002), Aerosol distributions and radiative properties simulated in the GOCART model and comparisons with observations, *J. Atmos. Sci.*, *59*, 461–483.

Chin, M., et al. (2004), Aerosol distribution in the Northern Hemisphere during ACE-Asia: Results from global model, satellite observations, and Sun photometer measurements, *J. Geophys. Res.*, *109*, D23S90, doi:10.1029/2004JD004829.

Chu, D. A., et al. (2005), Evaluation of aerosol properties over ocean from Moderate Resolution Imaging Spectroradiometer (MODIS) during ACE-Asia, *J. Geophys. Res.*, *110*, D07308, doi:10.1029/2004JD005208.

Christopher, S. A., and T. A. Jones (2007), Satellite-based assessment of cloud-free net radiative effect of dust aerosols over the Atlantic Ocean, *Geophys. Res. Lett.*, *34*, L02810, doi:10.1029/2006GL027783.

Christopher, S. A., J. Zhang, Y. J. Kaufman, and L. A. Remer (2006), Satellite-based assessment of top of atmosphere anthropogenic aerosol radiative forcing over cloud-free oceans, *Geophys. Res. Lett.*, *33*, L15816, doi:10.1029/2005GL025535.

Deeter, M. N., et al. (2003), Operational carbon monoxide retrieval algorithm and selected results for the MOPITT instrument, *J. Geophys. Res.*, *108*(D18), 4399, doi:10.1029/2002JD003186.

Edwards, D. P., et al. (2004), Observations of carbon monoxide and aerosols from the Terra satellite: Northern Hemisphere variability, *J. Geophys. Res.*, *109*, D24202, doi:10.1029/2004JD004727.

Hsu, C. N., J. R. Herman, and C. Weaver (2000), Determination of radiative forcing of Saharan dust using combined TOMS and ERBE data, *J. Geophys. Res.*, *105*(D16), 20,649–20,661.

Kalnay, E., et al. (1996), The NCEP/NCAR 40–year reanalysis project, *Bull. Am. Meteorol. Soc.*, *77*, 437–471.

Kaufman, Y. J., A. Smirnov, B. N. Holben, and O. Dubovik (2001), Baseline maritime aerosol: Methodology to derive the optical thickness and scattering properties, *Geophys. Res. Lett.*, *28*, 3251–3254.

Kaufman, Y. J., O. Boucher, D. Tanré, M. Chin, L. A. Remer, and T. Takemura (2005a), Aerosol anthropogenic component estimated from satellite data, *Geophys. Res. Lett.*, *32*, L17804, doi:10.1029/2005GL023125.

Kaufman, Y. J., I. Koren, L. A. Remer, D. Tanré, P. Ginoux, and S. Fan (2005b), Dust transport and deposition observed from the Terra-Moderate Resolution Imaging Spectroradiometer (MODIS) spacecraft over the Atlantic Ocean, *J. Geophys. Res.*, *110*, D10S12, doi:10.1029/2003JD004436.

Kleidman, R. G., et al. (2005), Comparison of Moderate Resolution Imaging Spectroradiometer (MODIS) and Aerosol Robotic Network (AERONET) remote-sensing retrievals of aerosol fine mode fraction over ocean, *J. Geophys. Res.*, *110*, D22205, doi:10.1029/2005JD005760.

Koch, D., T. C. Bond, D. Streets, N. Unger, and G. R. van der Werf (2007), Global impacts of aerosols from particular source regions and sectors, *J. Geophys. Res.*, *112*, D02205, doi:10.1029/2005JD007024.

Myhre, G., et al. (2004), Intercomparison of satellite retrieved aerosol optical depth over the ocean, *J. Atmos. Sci.*, *61*, 499–513, doi:10.1175/1520-0469(2004)061<0499:IOSRAO>2.0.CO;2.

Prospero, J. M., P. Ginoux, O. Torres, and S. Nicholson (2002), Environmental characterization of global sources of atmospheric soil dust derived from NIMBUS-7 TOMS absorbing aerosol product, *Rev. Geophys.*, *40*(1), 1002, doi:10.1029/2000RG000095.

Ramana, M. V., and V. Ramanathan (2006), Abrupt transition from natural to anthropogenic aerosol radiative forcing: Observations at the ABC-Maldives Climate Observatory, *J. Geophys. Res.*, *111*, D20207, doi:10.1029/2006JD007063.

Reid, J. S., R. Koppmann, T. F. Eck, and D. P. Eleuterio (2005), A review of biomass burning emissions part II: Intensive physical properties of biomass burning particles, *Atmos. Chem. Phys. Disc.*, *5*, 5201–5260.

Remer, L. A., and Y. J. Kaufman (2005), Aerosol effect on the distribution of solar radiation over the clear-sky global oceans derived from four years of MODIS retrievals, *Atmos. Chem. Phys. Disc.*, *5*, 5007–5038.

Remer, L. A., et al. (2005), The MODIS aerosol algorithm, products, and validation, *J. Atmos. Sci.*, *62*, 947–973.

Remer, L. A., D. Tanre, and Y. Kaufman (2006), Algorithm from Remote Sensing of Tropospheric Aerosol from MODIS: Collection 5, NASA Goddard Space Flight Cent., Greenbelt, Md. (Available at http://modis-atmos.gsfc.nasa.gov/MOD04_L2/atbd.html)

Tanré, D., et al. (2001), Climatology of dust aerosol size distribution and optical properties derived from remotely sensed data in the solar spectrum, *J. Geophys. Res.*, *106*, 18,205–18,217.

Torres, O., P. K. Bhartia, J. R. Herman, A. Sinyuk, P. Ginoux, and B. N. Holben (2002), A long-term record of aerosol optical depth from TOMS observations and comparison to AERONET measurements, *J. Atmos. Sci.*, *59*(3), 398–413.

Yu, H., et al. (2006), A review of measurement-based assessment of aerosol direct radiative effect and forcing, *Atmos. Chem. Phys. Disc.*, *5*, 7647–7768.

Zhang, J., and J. S. Reid (2006), MODIS aerosol product analysis for data assimilation: Assessment of over-ocean level 2 aerosol optical thickness retrievals, *J. Geophys. Res.*, *111*, D22207, doi:10.1029/2005JD006898.

S. A. Christopher and T. A. Jones, Department of Atmospheric Sciences, University of Alabama in Huntsville, Huntsville, AL 35806, USA. (tjones@nsstc.uah.edu)